

Patient-specific multiporoelastic brain modelling

Liwei Guo¹, John C. Vardakis¹, Dean Chou², Brett J. Tully³, Toni Lassila⁴, Nishant Ravikumar⁴, Zeike A. Taylor⁴, Susheel Varma⁴, Annalena Venneri^{5,6}, Alejandro F. Frangi⁴, Yiannis Ventikos^{1,*}

1 Department of Mechanical Engineering, University College London, UK

2 Institute of Biomedical Engineering & Department of Engineering Science, University of Oxford, UK

3 First Light Fusion Ltd., Begbroke Science Park, Begbroke, UK

4 Centre for Computational Imaging and Simulation Technologies in Biomedicine (CISTIB), Department of Electronic and Electrical Engineering, University of Sheffield, UK

5 Department of Neuroscience, Medical School, University of Sheffield, UK

6 IRCCS San Camillo Foundation Hospital, Venice, Italy

* Correspondence: y.ventikos@ucl.ac.uk, Department of Mechanical Engineering, University College London, Torrington Place, London WC1E 7JE, UK.

1. Introduction

The capability to model transport of the fluid content of the brain, in a personalised manner and from first principles, is essential for enhancing the biomechanical understanding of functional features like perfusion and clearance. This understanding is expected to yield novel information (and novel biomarkers) especially regarding early stages of diseases of old age, such as dementia.

The focus of this paper is to present a workflow within the VPH-DARE@IT Clinical Research Platform that can serve this purpose, i.e. to model the biomechanical behaviour of perfused brain tissue. This workflow features a 3D multiporoelastic framework, patient-specific brain anatomy representations and continuous waveforms of internal carotid and vertebral arteries, which are used as a means of personalising the boundary conditions. In the following sections, first the details of the integrated workflow will be introduced in Section 2, and then results of the 3D multiporoelastic modelling when incorporating patient-specific cerebroventricular system and parenchymal tissue geometry in addition to the artery waveforms will be shown in Section 3. Last, some brief discussion and conclusions are given in Section 4.

2. Materials and Methods

In this work, the multiple-network poroelastic theory (MPET) [1] is used to describe the transfer of fluid through the brain parenchyma. For a well-defined poroelastic medium, an equilibrium equation is needed to define elastic deformation; Darcy's law is used to model fluid flow; and finally mass conservation is also required. Here, the solid porous matrix represents brain parenchyma, whilst the communicating fluid phases that will be taken into account are: a high pressure arterial network (a), a lower pressure arteriole/capillary network (c), an extracellular/CSF network (e) and a venous network (v) (see Fig. 1).

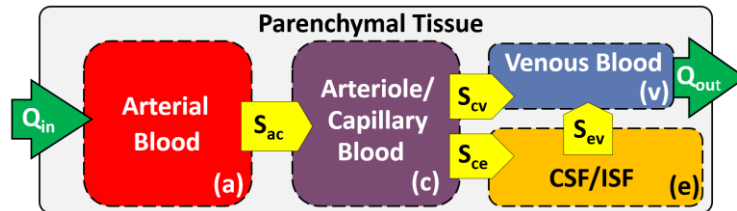


Figure 1: The four-compartment MPET model. Flow is prohibited between the CSF and the arterial network, whilst directional transfer exists between (a) and (c), (c) and (v), (c) and (e) and finally (e) and (v).

To solve this coupled system, we cast equations for the displacement of the solid matrix, \mathbf{u} , and the pore pressures of the four-compartment porous medium (p_a, p_c, p_e, p_v). The governing equations are listed below (Eq. 1 – 5) and they are discretized using the finite element method in our in-house solver.

$$G\nabla^2 \mathbf{u} + (G + \lambda)\nabla \varepsilon = (\alpha_a \nabla p_a + \alpha_c \nabla p_c + \alpha_e \nabla p_e + \alpha_v \nabla p_v) - \mathbf{F} \quad (1)$$

$$S_a^{-1} \frac{\partial p_a}{\partial t} + \alpha_a \frac{\partial \varepsilon}{\partial t} = \frac{k_a}{\mu_a} \nabla^2 p_a + (\hat{s}_{c \rightarrow a} + \hat{s}_{e \rightarrow a} + \hat{s}_{v \rightarrow a}) \quad (2)$$

$$S_c^{-1} \frac{\partial p_c}{\partial t} + \alpha_c \frac{\partial \varepsilon}{\partial t} = \frac{k_c}{\mu_c} \nabla^2 p_c + (\hat{s}_{a \rightarrow c} + \hat{s}_{e \rightarrow c} + \hat{s}_{v \rightarrow c}) \quad (3)$$

$$S_e^{-1} \frac{\partial p_e}{\partial t} + \alpha_e \frac{\partial \varepsilon}{\partial t} = \frac{k_e}{\mu_e} \nabla^2 p_e + (\hat{s}_{a \rightarrow e} + \hat{s}_{c \rightarrow e} + \hat{s}_{v \rightarrow e}) \quad (4)$$

$$S_v^{-1} \frac{\partial p_v}{\partial t} + \alpha_v \frac{\partial \varepsilon}{\partial t} = \frac{k_v}{\mu_v} \nabla^2 p_v + (\hat{s}_{a \rightarrow v} + \hat{s}_{c \rightarrow v} + \hat{s}_{e \rightarrow v}) \quad (5)$$

In order to ascertain the accuracy of the 3D MPET poroelastic solver, the numerical code is verified against two consolidation problems, i.e. Terzaghi's [2] and Mandel's [3] problems, respectively. In both of these simulations, a special case of the MPET system is utilised, specifically that of using a single compartment. It can be seen from Fig. 2 and 3 that the numerical results agree with the analytical solutions very well.

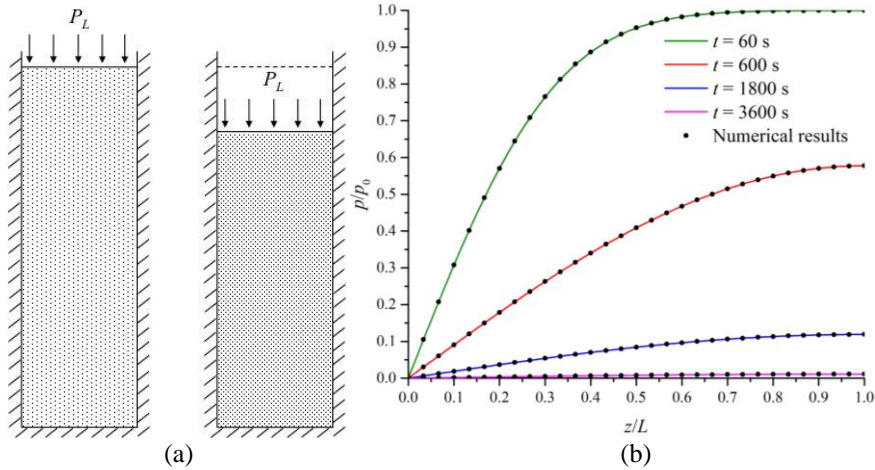


Figure 2: Terzaghi's consolidation problem. (a) Schematic description. (b) Plots of dimensionless pore pressure against dimensionless vertical distance. Coloured solid lines represent the analytical solutions.

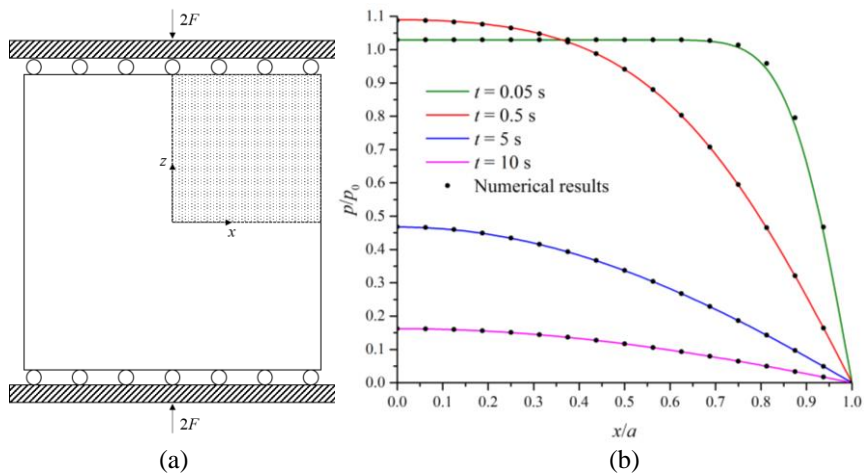


Figure 3: Mandel's consolidation problem. (a) Schematic description. (b) Plots of dimensionless pore pressure against dimensionless horizontal distance from the centre. Coloured solid lines represent the analytical solutions.

In addition to the 3D MPET poroelastic solver, patient-specific geometry (image acquisition, segmentation, surface correction and smoothing, and mesh generation) is utilised in combination with waveforms of arterial blood flow profiles for patient-specific modelling. The integrated workflow

depicted in Fig. 4 is able to take patient-specific measurements of internal carotid and vertebral artery (ICA and VA) flow in both left and right sides of the cerebrum and cerebellum as input conditions in the numerical modelling and calculate output, such as fluid pressure, tissue deformation and perfusion map.

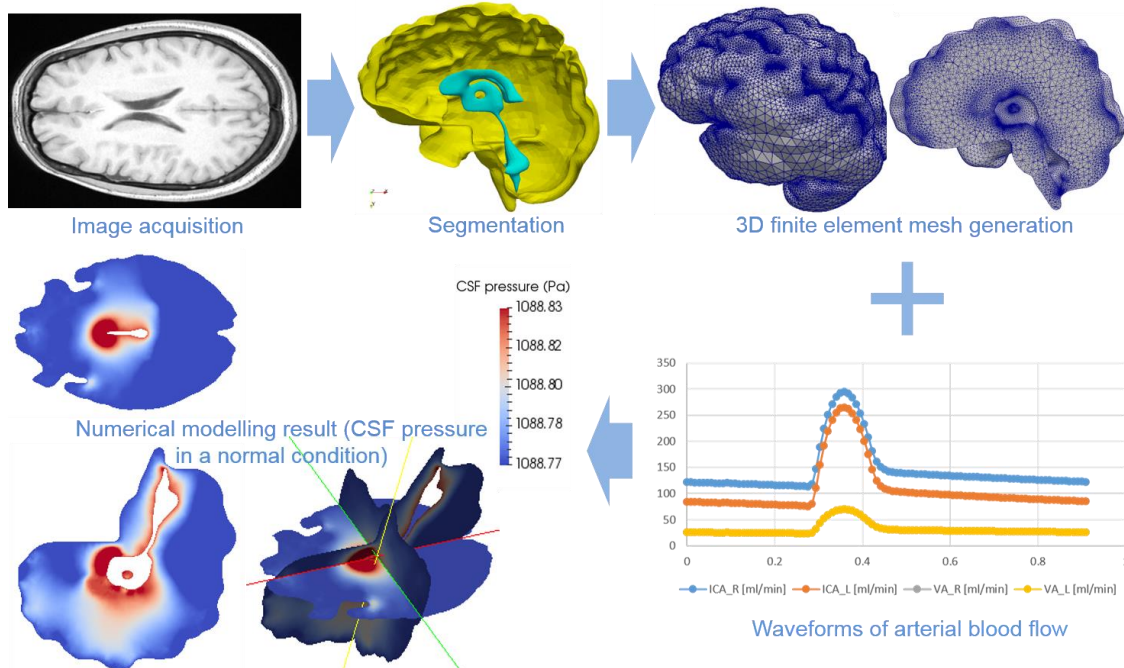


Figure 4: The workflow that incorporates the 3D MPET solver, image segmentation and meshing, and the arterial boundary conditions.

3. Results

In this section, one MCI (Mild Cognitive Impairment) patient and one control case (both female, 82 years old) are selected as examples to show the modelling results obtained from the integrated workflow. Patient-specific cerebroventricular system and parenchymal tissue geometry are used to create the meshes for finite element modelling; patient-specific internal carotid and vertebral artery waveforms are applied as boundary conditions for the arterial compartment and traditional boundary conditions from the literature [4] are applied on the other three compartments (the arteriole/capillary compartment, the extracellular/CSF compartment and the venous compartment), however they can incorporate the same flexibility in adopting patient-specific boundary conditions if data are available.

The pressure (unit: Pa) fields of the arterial compartment, which is the compartment that accepts the feeding patient-specific flow boundary conditions are shown in Fig. 5a and e, and the intracranial pressure contours (ICP, unit: Pa) are shown in Fig. 5b and f. Fig. 5c and g show the displacement magnitude of the parenchymal tissue (unit: m), which incorporates the pressure gradients of the aforementioned, patient-specific arterial compartment. Last, the perfusion maps (unit: m/s) of the capillary compartment are shown in Fig. 5d and h.

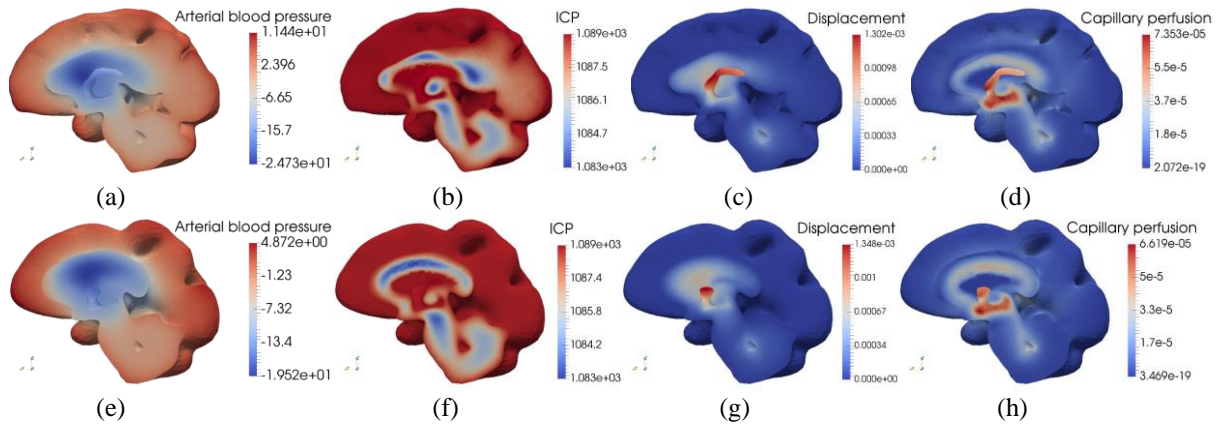


Figure 5: Numerical modelling results of one control case (a – d) and one MCI patient (e – h) on sagittal planes.

4. Discussion and Conclusions

It can be seen from the result section that for this pair of MCI and control cases, there is reduced capillary perfusion in the MCI case, whilst a high arterial blood pressure is maintained due to the higher magnitude of the arterial blood flow (as input boundary conditions) compared with the control case. The peak parenchymal tissue displacement is also higher in the MCI case, possibly reflecting neuronal damage in tissue. It should be noted that these are only preliminary results based on two subjects; more data need to be analysed to find more concrete conclusions.

The workflow described in this paper allows for the simultaneous solution of personalized fluid transport of four interconnected compartments (arterial, capillary, CSF/ISF and venous), within a deformable solid matrix (parenchymal tissue). The application of the integrated workflow is shown in the form of some preliminary results, highlighting the application of the patient-specific brain geometry and boundary conditions of the arterial compartment. The integrated workflow described in this paper is now being used on a large number of subjects for identifying novel information (and novel biomarkers). This will be especially useful for the early stages of dementia, where, possibly, variation from normal conditions, too subtle to be captured directly via imaging, can be characterised and correlated with clinical findings.

5. References

1. Tully BJ et al., *J. Fluid Mech.* 2011;667:188-215
2. Terzaghi K, *Erdbaumechanik auf Bodenphysikalischer Grundlage*. Vienna, F. Duticke, 1925
3. Mandel J, *Géotechnique*. 1953;3(7):287-299
4. Vardakis JC et al., *PLoS ONE*. 2013;8(12):e84577